

# Sensitive molecular binding assay using a photonic crystal structure in total internal reflection

Yunbo Guo<sup>1,2</sup>, Charles Divin<sup>1,2</sup>, Andrzej Myc<sup>3</sup>, Fred L. Terry, Jr.<sup>2</sup>, James R. Baker, Jr.<sup>3</sup>, Theodore B. Norris<sup>1,2,3\*</sup>, and Jing Yong Ye<sup>1,2,3</sup>

<sup>1</sup>Center for Ultrafast Optical Science, University of Michigan, Ann Arbor, MI 48109-2099, USA

<sup>2</sup>Department of Electrical Engineering & Computer Science, University of Michigan, Ann Arbor, MI 48109-2122, USA

<sup>3</sup>Michigan Nanotechnology Institute for Medicine and Biological Sciences, University of Michigan, Ann Arbor, MI 48109-0648, USA

\*Corresponding author: [tnorris@eecs.umich.edu](mailto:tnorris@eecs.umich.edu)

**Abstract:** A novel optical sensor for label-free biomolecular binding assay using a one-dimensional photonic crystal in a total-internal-reflection geometry is proposed and demonstrated. The simple configuration provides a narrow optical resonance to enable sensitive measurements of molecular binding, and at the same time employs an open interface to enable real-time measurements of binding dynamics. Ultrathin aminopropyltriethoxysilane/glutaraldehyde films adsorbed on the interface were detected by measuring the spectral shift of the photonic crystal resonance and the intensity ratio change in a differential reflectance measurement. A detection limit of  $6 \times 10^{-5}$  nm for molecular layer thickness was obtained, which corresponds to a detection limit for analyte adsorption of  $0.06 \text{ pg/mm}^2$  or a refractive index resolution of  $3 \times 10^{-8}$  RIU; this represents a significant improvement relative to state-of-the-art surface-plasmon-resonance-based systems.

©2008 Optical Society of America

**OCIS codes:** (280.1415) Biological sensing and sensors; (230.5298) Photonic crystals; (260.6970) Total internal reflection.

---

## References and links

1. J. Homola, "Surface plasmon resonance sensors for detection of chemical and biological species," *Chem. Rev.* **108**, 462-493 (2008).
2. X. D. Hoaa, A. G. Kirk, and M. Tabrizian, "Towards integrated and sensitive surface plasmon resonance biosensors: A review of recent progress," *Biosensors and Bioelectronics* **23**, 151-160 (2007).
3. J. Homola, "Present and future of surface plasmon resonance biosensors," *Anal. Bioanal. Chem.* **377**, 528-539 (2003).
4. D. G. Myszka, X. He, M. Dembo, T. A. Morton, and B. Goldstein, "Extending the range of rate constants available from BIACORE: Interpreting mass transport-influenced binding data," *Biophys. J.* **75**, 583-594 (1998).
5. D. O'Shannessy, "Determination of Kinetic Rate and Equilibrium Binding Constants for Macromolecular Interactions: A Critique of the Surface Plasmon Resonance Literature," *Curr. Opin. Biotechnol.* **5**, 65-71 (1994).
6. R. Horvath, N. Skivesen, H. C. Pedersen, "Measurement of guided light-mode intensity: An alternative waveguide sensing principle," *Appl. Phys. Lett.* **84**, 4044-4046 (2004).
7. F. Vollmer, D. Braun, A. Libchaber, M. Khoshsima, I. Teraoka, and S. Arnold, "Protein Detection by Optical shift of a Resonant Microcavity," *Appl. Phys. Lett.* **80**, 4057-4059 (2002).
8. I. M. White, H. Oveys, X. Fan, T. L. Smith, and J. Zhang, "Integrated multiplexed biosensors based on liquid core optical ring resonators and antiresonant reflecting optical waveguides," *Appl. Phys. Lett.* **89**, 191106 (2006).
9. A. M. Armani, R. P. Kulkarni, S. E. Fraser, R. C. Flagan, and K. J. Vahala, "Label-Free, Single-Molecule Detection with Optical Microcavities," *Science* **317**, 783-787 (2007).
10. V. S. Ilchenko and M. L. Gorodetskii, "Thermal nonlinear effects in optical whispering gallery microresonators," *Laser Phys.* **2**, 1004-1009 (1992).
11. V. Mulloni, and L. Pavesi, "Porous silicon microcavities as optical chemical sensors," *Appl. Phys. Lett.* **76**, 2523-2525 (2000).
12. H. Ouyang, C. C. Striemer, and P. M. Fauchet, "Quantitative analysis of the sensitivity of porous silicon optical biosensors," *Appl. Phys. Lett.* **88**, 163108 (2006).
13. W. M. Robertson and M. S. May, "Surface electromagnetic wave excitation on one-dimensional photonic band-gap arrays," *Appl. Phys. Lett.* **74**, 1800-1802 (1999).

14. F. Villa, L. E. Regalado, F. Ramos-Mendieta, J. Gaspar-Armenta, and T. Lopez-Rios, "Photonic crystal sensor based on surface waves for thin-film characterization," *Opt. Lett.* **27**, 646-648 (2002).
15. B. A. Usievich, V. V. Svetikov, D. Kh. Nurligareev, and V.A. Sychugov, "Surface waves at the boundary of a system of coupled waveguides," *Quant. Electr.*, **37**, 981-984 (2007).
16. M. Shin and W. M. Robertson, "Surface plasmon-like sensor based on surface electromagnetic waves in a photonic band-gap material," *Sens. Actuators B* **105**, 360-364 (2005).
17. V. N. Konopsky and E. V. Alieva, "Photonic crystal surface waves for optical biosensors," *Anal. Chem.* **79**, 4729-4735 (2007).
18. J. Y. Ye and M. Ishikawa, "Light enhancement method and device, and their applications in fluorescence detection," Patent: JP 2001-242083.
19. H. Inouye, M. Arakawa, J. Y. Ye, T. Hattori, H. Nakatsuka, and K. Hirao, "Optical properties of a total-reflection-type one-dimensional photonic crystal," *IEEE J. Quant. Electr.* **38**, 867-871 (2002).
20. R. Kaiser, Y. Levy, N. Vansteenkiste, A. Aspect, W. Seifert, D. Leipold, and J. Mlynek, "Resonant enhancement of evanescent waves with a thin dielectric waveguide," *Opt. Commun.* **104**, 234-240 (1994).
21. O. Schmidt, P. Kiesel, S. Mohta, and N. M. Johnson, "Resolving pm wavelength shifts in optical sensing," *Appl. Phys. B*, **86**, 593-600 (2007).
22. B. Ran, and S. G. Lipson, "Comparison between sensitivities of phase and intensity detection in surface plasmon resonance," *Opt. Express* **14**, 5641-5650 (2006), <http://www.opticsinfobase.org/abstract.cfm?URI=oe-14-12-5641>.
23. X. B. Liu, Z. Q. Cao, Q. S. Shen, and S. Huang, "Optical Sensor Based on Fabry-Perot Resonance Modes," *Appl. Opt.* **42**, 7137-7140 (2003).
24. J. S. Shumaker-Parry, and C. T. Campbell, "Quantitative methods for spatially resolved adsorption/desorption measurements in real time by surface plasmon resonance microscopy," *Anal. Chem.* **76**, 907-917 (2004).
25. D. G. Myszka, "Improving biosensor analysis," *J. Mol. Recognit.*, **12**, 279-284 (1999).
26. Z. Knittl, *Optics of Thin films (An Optical Multilayer Theory)* (Wiley, London 1976).
27. G. T. Hermanson, *Biocojugate Techniques Academic* (Press, New York 1996).
28. L. S. Jung, C. T. Campbell, T. M. Chinowsky, M. N. Mar, and S. S. Yee, "Quantitative interpretation of the response of surface plasmon resonance sensors to adsorbed films," *Langmuir* **14**, 5636-5648 (1998).
29. C. E. Stewart, I. R. Hooper, and J. R. Sambles, "Surface plasmon differential ellipsometry of aqueous solutions for biochemical," *J. Phys. D: Appl. Phys.* **41**, 105408 (2008).

## 1. Introduction

Novel optical methods for performing binding assays have attracted growing attention driven by increasing demands for better understanding of specific interactions between biomolecules, which provide a chemical foundation for all cellular processes. The general approach is to exploit the shift or broadening of a resonant optical structure that occurs when the binding of analyte molecules to the structure modifies the local index of refraction. This approach is label-free, in contrast to fluorescence-based methods, and under some circumstances can provide information on binding dynamics as well as binding affinity. The most widely used assay utilizes the surface-plasmon resonance (SPR) effect [1-3], which works well for large analyte molecules with reasonably high binding affinities, and is employed in commercially available instruments. In order to achieve higher sensitivity, resonant optical cavities of various sorts have been employed (see below), but these structures suffer from limitations either of mass transport into the device, or from nontrivial coupling into high-Q resonant cavities. In this paper we present a novel optical structure that achieves significantly higher sensitivity than SPR-based devices, but involves a simple geometry and can measure real-time surface binding without mass transport limitations.

The study of biomolecular affinity and binding kinetics is of great importance for many fields in biomedical and pharmaceutical research. For example, one approach to the development of novel therapeutics is to screen a large repertoire of small molecules to identify high specificity and high affinity binders, followed by a more detailed characterization of the binding properties and determination of epitope specificity. Present SPR-based systems detect the binding of analytes to ligands immobilized on a metal surface by measuring the effect of the bound molecules on the index of refraction seen by the evanescent wave of the SPR mode. Although SPR has become the dominant optical tool for binding assays, the sensitivity of SPR-based detection is not sufficient for applications that require detection of small molecules or low surface coverage of bound molecules. In practice, the SPR method requires greater than 1 pg/mm<sup>2</sup> of analyte binding [1, 2], although it is very difficult to immobilize a sufficiently high density of ligand onto a surface to achieve this level of analyte binding. Thus, a 100-200 nm thick carboxymethylated dextran matrix is attached to the metal surface

in order to effectively add a third dimension to the surface and produce much higher levels of ligand immobilization [1]. Although this enables higher sensitivity to be achieved, the presence of this matrix gives rise to a mass transport problem, as the analyte molecules must diffuse into and out of the matrix during binding and unbinding. Indeed, the mass transport issue has raised questions about the validity of some of the published kinetic rates obtained from SPR measurements [4, 5]. Therefore, there is a need for optical devices that have higher sensitivity and at the same time are less susceptible to mass transport limitations.

The key to obtaining higher sensitivity is clearly to employ an optical resonance which is narrower than the (very broad) surface plasmon resonance. Recently the evanescent fields of optical modes in waveguides [6] and of whispering-gallery-mode (WGM) resonances [7-9] have been demonstrated for biosensing applications. These kinds of resonators can provide large evanescent fields and high Q-factors to enable high sensitivity. Microtoroid resonators using WGM resonances exhibit ultra-high Q values ( $>10^8$ ) and are able to detect adsorption of single molecules [9]. Although very-high-Q resonators provide the ultimate sensitivity, they generally have the drawbacks that coupling light into and out of the resonators can be challenging, and from sensitivity to thermal instability [10].

Fabry-Perot microcavities or similar one-dimensional photonic-crystal structures (1-D PCs) have also been investigated as optical biosensors. Specifically, microcavities fabricated from multilayers of porous silicon have been developed [11, 12]; because the position of the cavity resonance is critically dependent on the index of refraction of the layers, adsorption of analyte molecules onto the porous silicon surfaces results in a measurable shift in the resonance, enabling sensitive detection. Although the porous-silicon biosensor provides higher sensitivity than SPR-based sensors, it is not possible to measure real-time binding kinetics due to the slow diffusion of biomolecules into the sub-micron pores.

In order to enable real-time binding measurements, one requires an open surface, which can be accessed optically via an evanescent wave. One approach is to employ a surface electromagnetic wave (SEW) excited in a Kretschmann-like geometry [13]. Basically, in total internal reflection, light of all frequencies is reflected, and no useful resonance appears which can be used for sensing. An energy loss mechanism is required, and in the case of the SEW there is a natural mechanism for energy loss via tunneling of localized bulk excitations [14]. This SEW mode in essence comes from the violation of a uniform waveguide system caused by edge effects [15], so the structure is normally an incomplete layer on top of a 1-D PCs [14, 16]. The SEW mode is confined in the evanescent region and propagates along the interface, and is highly sensitive to the incomplete layer, which has been used for sensor applications [14, 16, 17].

In this letter, we present another novel sensor using a one-dimensional PC structure in a total internal reflection (TIR) geometry (PC-TIR sensor). The principle behind the appearance of the resonance in our structure has some important differences from SEW devices. Instead of an incomplete layer without absorption on top of a 1-D PCs in the SEW sensor, the resonance mode of our PC-TIR sensor is due to an intentionally inserted absorbing layer in the defect region of the PC structure. There is no surface-propagating wave present. The resonant PC structure defines a wavelength range over which the field is enhanced in the defect region, thus leading to selective absorption and the appearance of a resonance. This approach has a significant advantage in that the absorption can be engineered to yield an optimum resonance – i.e. an extra and highly controllable degree of freedom is available in the design. Local electrical field enhancement in such a structure has been observed by fluorescence experiments [18, 19]. Here we will demonstrate its application to biomolecular binding detection. As discussed below, this PC-TIR sensor functions as a Fabry-Perot resonator, yielding a sharper resonance than the SPR sensor and hence a higher detection sensitivity, and yet the surface available for analyte binding is open to free space to eliminate mass-transport issues and allow real-time binding measurements. This configuration possesses the advantages of evanescent-field-based optical resonators without light coupling problems as the cavity Q is not made too large. Moreover, the properties of PC structures make it easy to be designed and engineered to operate at any optical wavelength.

## 2. Principle

Figure 1 shows the design principle of the PC-TIR biosensor. In order to enable analyte molecules to access the sensing surface, we conceptually split a Fabry-Perot cavity (Fig. 1(a)) in half; in other words, the resonator consists of a high-reflecting PC structure and a single defect layer (Fig. 1(c)). Light is incident through a coupling prism at an angle greater than the angle for TIR. Owing to the TIR, the light propagation may be thought of in terms of an imaginary PC structure (Fig. 1(b)), forming a microresonator. For light that is resonant with the cavity mode, the optical field will be enhanced near the surface of the defect layer; light outside the photonic bandgap is reflected from the PC layers and has a reduced field amplitude at the surface. Of course, light of all frequencies would be reflected from such a structure, so we incorporate a small amount of absorbing material in the defect layer; only light resonant with the microcavity mode will be absorbed in this layer. Thus the reflectance spectrum of the total PC-TIR structure will show a pronounced dip at the resonant frequency, whose smallest reflectance can be engineered to be nearly zero by optimizing the absorption in the defect layer [19].

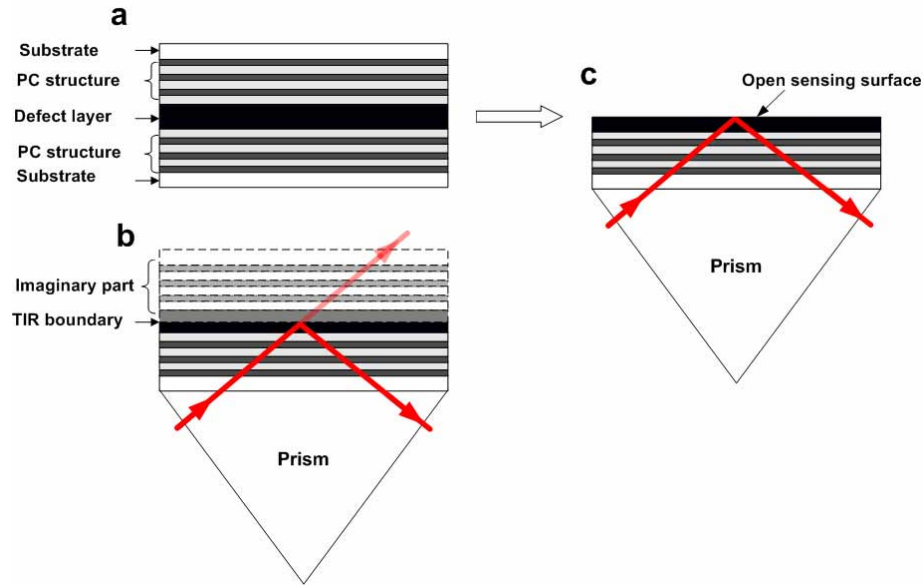


Fig. 1. Principle of a PC-TIR sensor. (a), A sample sandwiched by two pieces of PC structures. We conceptually split this structure from the middle layer into two pieces. (b), Use only one piece of the PC structure in a TIR geometry. Owing to the TIR, conceptually an imaginary PC structure exists and forms a microcavity as if there would be two pieces of PC structures. (c), This PC-TIR sensor offers a unique sensing interface open for biomolecular assay.

The operating principle of a PC-TIR sensor is as follows. Assume the incident angle at the substrate layer is  $\theta_s$ , and the refraction angles in the lower index layer, higher index layer, and the defect layer are  $\theta_a$ ,  $\theta_b$ , and  $\theta_x$ , respectively. Let  $n_s$ ,  $n_a$ ,  $n_b$ , and  $n_x$  be the refractive index of the substrate, lower index layer, higher index layer, and the defect layer, respectively. According to Snell's law,

$$n_s \sin \theta_s = n_a \sin \theta_a = n_b \sin \theta_b = n_x \sin \theta_x \quad (1)$$

In order to form the photonic crystal structure, the properties of dielectric multilayers should satisfy

$$n_a d_a \cos \theta_a = n_b d_b \cos \theta_b = \lambda_r / 4 \quad (2)$$

where  $\lambda_R$  is the resonant wavelength,  $d_a$ ,  $d_b$  represent the physical thickness of the low and high index layers, respectively.

The thickness of the defect layer,  $d_x$ , is determined by the following resonant condition,

$$2 \cdot \frac{2\pi}{\lambda_R} n_x d_x \cos \theta_x + \alpha = (2m+1)\pi \quad (m=0,1,2,\dots) \quad (3)$$

where  $\alpha$  represents the Goos-Hänchen phase shift between the defect layer and bulk medium. The factor of 2 in the first term on the left hand side is due to the fact that the light double passes the defect layer owing to the TIR.

If analyte molecules bind to ligands on the surface of the defect layer, they will give rise to a shift in the cavity resonance due to the phase shift seen by light propagating in the defect layer and undergoing TIR. Because of the field enhancement near the surface and the high Q of the microcavity, the shift can be very sensitive to molecular binding. The key feature of the PC-TIR sensor is that the surface available for binding is open, thus reducing mass transport limitations, and the cavity Q can be optimized through the design of the PC multilayer structure. As with the SPR sensor, the analytes bound to the sensing surface do not need to absorb the light and the method is label-free.

The adlayer binding to the sensing surface will change the resonant condition to:

$$2 \cdot \frac{2\pi}{\lambda_R'} (n_x d_x \cos \theta_x + n_{ad} d_{ad} \cos \theta_{ad}) + \alpha' = (2m+1)\pi \quad (m=0,1,2,\dots) \quad (4)$$

where  $n_{ad}$ ,  $d_{ad}$  and  $\theta_{ad}$  are the refractive index, thickness and refracted angle of the adlayer, respectively.  $\lambda_R'$  represent the new resonance wavelength, and  $\alpha'$  is the effective Goos-Hänchen phase shift after the adlayer binding [20].

Therefore, by monitoring the reflectance response, one can detect the properties of binding biomolecules (e.g. physical thickness or refractive index). There are two methods to measure the shift of the resonance dip. The first is to measure the resonance wavelength shift using a white light source and a spectrometer. However, the detection sensitivity is limited, mainly by the spectrometer resolution [21]. Much higher sensitivity can be obtained by performing an intensity measurement with a narrow-band optical probe tuned to the edge of the resonance line [21-24]. When a single-wavelength probe light is tuned near the half-width of the resonance dip, the reflected beam intensity varies sensitively with the analyte binding on the sensing surface due to the shift of the resonance dip wavelength  $\lambda_R$ .

The overall sensitivity  $S$  of the PC-TIR sensor using the intensity detection approach depends on two figures of merit: the conversion efficiency of resonant wavelength shift to the change of the intensity  $I_r$  (optical sensitivity  $O_s$ ) and the conversion efficiency of molecular binding to resonant wavelength shift (binding sensitivity  $B_s$ ). The latter term  $B_s$  is a function of the thickness ( $d_{ad}$ ) and refractive index ( $n_{ad}$ ) of the adlayer bound to the sensing surface; here we emphasize its relation with the adlayer thickness  $d_{ad}$ , and presume that the adlayer has essentially the same refractive index as the sensing surface:

$$S = \frac{\partial I_r}{\partial d_{ad}} = \frac{\partial I_r}{\partial \lambda_R} \cdot \frac{\partial \lambda_R}{\partial d_{ad}} = O_s \cdot B_s \quad (5)$$

which indicates that the overall sensitivity  $S$  of the PC-TIR sensor is given by the product of  $O_s$  and  $B_s$ .

Since the resonance of the PC-TIR sensor is a Fabry-Perot cavity mode, its reflectance spectrum near the resonance can be described by Lorentz curve as

$$I_r = I_0 \left[ 1 - \frac{1 - R_{\min}}{1 + \left( \frac{\lambda_R - \lambda_0}{\Delta\lambda/2} \right)^2} \right] \quad (6)$$

where  $I_0$  is the incident probe light intensity,  $R_{min}$  is the minimum reflectance of the resonant dip,  $\lambda_0$  is the initial resonance wavelength and  $\Delta\lambda$  is the full width at half maximum (FWHM) of the resonance dip.

When  $\lambda_R = \lambda_0 \pm 0.29\Delta\lambda$ , the maximum optical sensitivity  $O_{s,max}$  can be obtained

$$O_{s,max} = \left( \frac{\partial I_r}{\partial \lambda_R} \right)_{max} = \pm \frac{1.3I_0(1-R_{min})}{\Delta\lambda} \quad (7)$$

The positive (negative) sign corresponds to the probe light wavelength lying on the lower (upper) side of the resonant dip.

According to Equation (4), with the assumption  $n_{ad} = n_x$ , there is  $\alpha' = \alpha$ , and the binding sensitivity  $B_s$  can be expressed as

$$B_s = \frac{4\pi n_{ad} \cos \theta_{ad}}{(2m+1)\pi - \alpha} \quad (8)$$

Substituting Equations (7) and (8) into Equation (5), one obtains the maximum overall sensitivity,

$$S_{max} = \pm \frac{5.2\pi n_{ad} \cos \theta_{ad} I_0(1-R_{min})}{[(2m+1)\pi - \alpha] \Delta\lambda} \quad (9)$$

Because the minimum reflectance  $R_{min}$  can be nearly 0 by optimizing the absorption in the defect layer, and smaller resonance dip width  $\Delta\lambda$  can be easily obtained by increasing the number of the dielectric layers in the PC structure, the intensity detection mode may be used rather than the full spectral measurement in order to take the advantage of the narrow resonance dip of a PC-TIR microcavity and achieve the highest possible sensitivity. Of course, Equation (9) also implies that intensity fluctuations of the incident probe light directly affect the PC-TIR sensor response. Thus a differential reflectance method is required to suppress the effect of laser fluctuations [25]. As illustrated in Figure 2, a HeNe probe laser beam was split into two and the ratio of the light intensity reflected from a binding area to a reference area of the sensor was measured.

### 3. Experiment

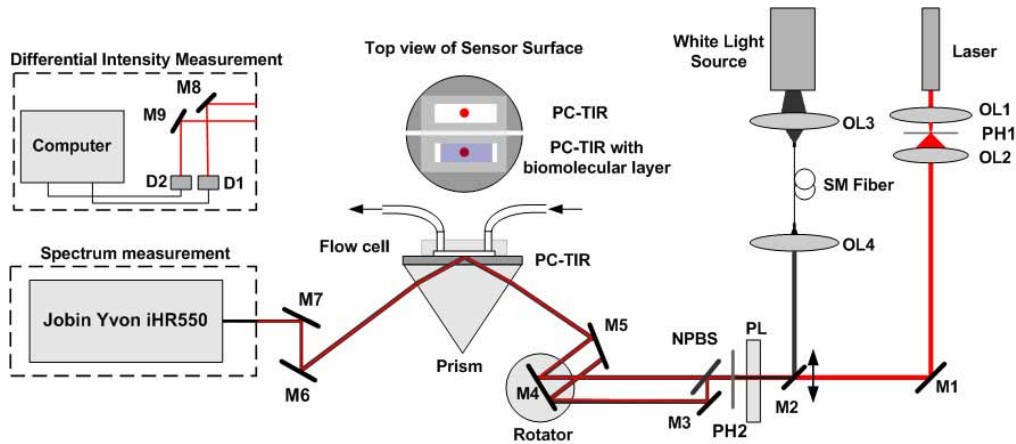


Fig. 2. Experimental setup for spectral detection and differential reflectance measurements. OL1-OL5: objective lenses, PH1-PH2: pinhole, PL: polarizer, NPBS: Non-polarizing beam splitter, M1-M9: reflecting mirrors, D1-D2: photodiode detectors.

Figure 2 shows the experimental setup which combines the white light spectral measurement and the laser intensity measurement. For spectral measurement, a white light source is used. The beam was coupled with an objective lens into a single-mode optical fiber to obtain a good spatial beam profile and was collimated with a second objective lens. A linear polarizer was

used to select TE polarized light, and a 1-mm pinhole (PH2) was used to set the size of the probe beam. The beam was incident on the PC-TIR sensor with an incident angle controlled using a high precision programmed rotation stage. The reflected beam was propagated into a spectrometer (Jobin Yvon iHR550) with a resolution of 0.025 nm to measure the reflectance spectrum around the resonance dip. For intensity measurement, a single wavelength laser (HeNe laser) was used and the collimated laser beam traveled the same path as the white light except that the reflected light was directly detected using a pair of photodiode detectors. These two measurements could be easily switched by moving mirror M2, which enabled us to monitor the molecular binding with spectral shift and intensity ratio change almost concurrently.

Figure 3(a) shows a schematic of the structure of a PC-TIR sensor used in this study. The PC structure is composed of pairs of alternating 106-nm  $\text{TiO}_2$  and 334-nm  $\text{SiO}_2$  layers. A 20-nm Si thin layer was used as the absorptive layer and formed the defect layer with a 330-nm  $\text{SiO}_2$  layer. The dielectric layers were coated by electron-beam deposition onto a BK-7 glass substrate with flatness of  $\lambda/10$ . The thicknesses of these layers were designed using a transfer matrix method [26] to achieve minimum reflectance by incorporating appropriate absorption in the defect layer. The sensor was placed on a prism with refractive index matching oil.

Figure 3(b) shows the reflectance spectra of the PC-TIR sensor when the incident angle in the substrate is  $63.59^\circ$  and the top sensing surface is covered by de-ionized (DI) water. The reflectance dip is in reasonable agreement with a simulation using a transfer matrix calculation [26]. It has a resonance wavelength of 638.17nm and a narrow resonance width  $\Delta\lambda$  of 1.30 nm. Although the resonance width is slightly larger than the simulated value of 0.60 nm due to nonuniformity of the deposited thin films, it is much narrower than that of a typical SPR resonance (about 40 nm)[3], and allows more sensitive detection of resonance shifts. In addition, Fig. 3(b) also shows that the reflectance spectrum near the resonance can be well-fit by a Lorentzian lineshape. By adjusting the incident angle, one can tune the resonance dip to the desired wavelength. For the experiments reported here, the incident angle was adjusted to  $63.74^\circ$  to tune the resonant wavelength to 632.0nm, so that a HeNe laser at 632.8 nm lies in the linear region of the resonant dip [23, 24] and could be used to detect the resonance shift with molecular binding.

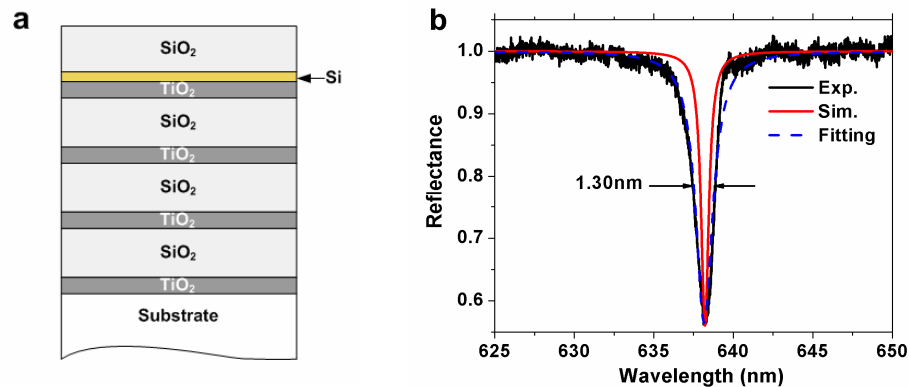


Fig. 3. (a), PC-TIR sensor structure. (b), Experimental, simulated and Lorentz fitting PC-TIR reflectance spectra.

To demonstrate the operation of the PC-TIR sensor, and to determine its sensitivity, we used two coupling agents, aminopropyltriethoxysilane (APTES) and glutaraldehyde, which can form uniform thin layers on silica surfaces [27]. The sensing surface was first cleaned by a piranha solution ( $\text{H}_2\text{SO}_4$  (95%) /  $\text{H}_2\text{O}_2$  (30%) = 3:1), and then a flow cell with two channels formed of PDMS is placed on top of the surface. Solutions are introduced to the sensing surface by withdrawing syringes controlled by a syringe pump. The binding procedure used here was similar to that described in Reference [12]. Briefly, the sensing surface was first

exposed to 5% APTES in H<sub>2</sub>O and methanol (1:1) solution for 20 minutes, then rinsed with de-ionized (DI) water and dried with air. After the silanization, a thin layer of APTES molecules was formed on the sensing surface. Then the sensor was exposed to a 2.5% glutaraldehyde solution in 20 mM HEPES buffer (pH=7.4) for 30 minutes and rinsed with DI water and dried with air. A thin layer of glutaraldehyde molecules was adsorbed on the surface due to the reaction with the amino groups on the silanized surface.

We performed spectroscopic ellipsometry measurements on a separate substrate (a crystalline p-type silicon wafer with a thin thermally oxidized layer of thickness  $4.93 \pm 0.02$  nm) to provide an independent determination of the layer thicknesses; we found the APTES monolayer and APTES/glutaraldehyde bilayer to be  $0.55 \pm 0.04$  nm and  $1.31 \pm 0.04$  nm respectively, assuming the refractive indices of APTES and glutaraldehyde to be 1.46 [12].

The shift of the PC-TIR resonance as the layers were adsorbed was first observed by measuring the reflectance spectrum. The results, shown in Figure 4(a), revealed a resonant wavelength shift of 0.52 and 1.18 nm respectively as the APTES monolayer and APTES/glutaraldehyde bilayer were formed. With the refractive indices of APTES and glutaraldehyde assumed to be 1.46, their physical thicknesses adsorption on the sensing surface are calculated to be 0.62 and 1.39 nm from the transfer matrix simulation [26], which are in approximate agreement with the ellipsometry measurement.

In addition, the differential reflectance ratio change was observed. Taken as a reference point, the ratio for the bare PC-TIR sensor changed from 1.00000 to 0.77814 for the binding of an APTES monolayer (data in Figure 4(b)). Since the probe laser wavelength 632.8 nm shifted out of the linear region of the resonant dip when the glutaraldehyde layer was formed, the ratio change for this layer is not a meaningful quantity.

Similar to SPR-based systems, our present experimental setup is characterized by a short term noise floor and a long term drift limited by the detection electronics and the mechanical stability of the system, respectively. Over a typical molecular binding period (150 seconds) [7, 17, 25], with a 1-Hz signal bandwidth, both the differential reflectance noise floor (i.e., standard deviation) and long term drift are below  $2.5 \times 10^{-5}$ . Assuming this as the smallest detectable signal, the detection limit of our PC-TIR sensor for analyte layer thickness is thus estimated to be  $0.55 \text{ nm} \times (2.5 \times 10^{-5} / 0.22186) = 6 \times 10^{-5} \text{ nm}$ , as the ratio changed by 0.22186 for a 0.55-nm APTES monolayer. This thickness detection limit corresponds to  $10^{-4}$  monolayers or  $0.06 \text{ pg/mm}^2$  for an analyte such as APTES which has a bulk density  $0.946 \text{ g/cm}^3$  [24, 28]. Moreover, the detection limit corresponds to a resonant wavelength shift  $5 \times 10^{-5} \text{ nm}$ . With the sensitivity for solvent refractive index change measured to be 1490 nm/RIU, our PC-TIR sensor also has a detection limit of  $3 \times 10^{-8}$  RIU, which represents an order-of-magnitude improvement over conventional SPR based measurements [1, 2, 29]. We note that the resonance width of the PC-TIR sensor can be made much narrower by increasing the number and uniformity of dielectric layers in the structure, in contrast to a fixed SPR bandwidth of a metal film.



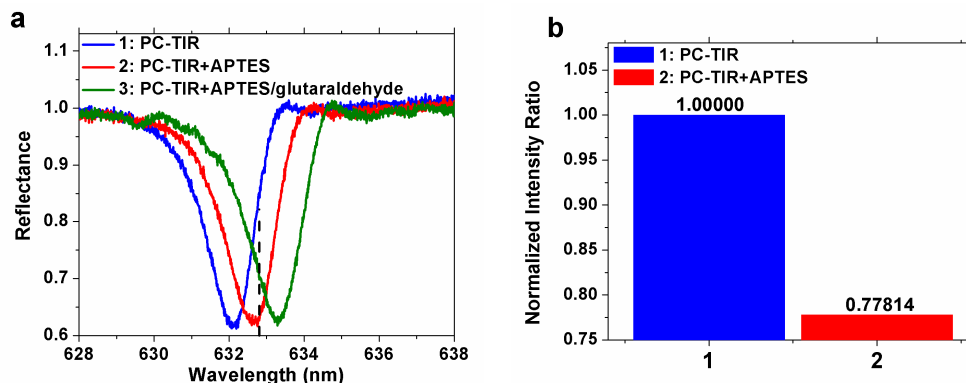


Fig. 4. (a), Resonance dip wavelength shifts with the binding of adlayer. (b), Reflectance ratios at 632.8 nm from differential reflectance measurements for a PC-TIR sensor without treatments (blue) and with APTES monolayer (red).

#### 4. Conclusion

To summarize, we have proposed a novel biosensor based on a PC structure used in a TIR configuration. We have demonstrated the operation of the sensor and determined its detection limit by observing the binding of an APTES monolayer and APTES/glutaraldehyde bilayer. Of course, for detection of biologically important ligands, other surface functionalizations may be used. The PC-TIR sensor provides an open interface allowing easy access for sensitive real-time binding assays. A significantly improved detection limit was experimentally shown for the PC-TIR sensor in comparison with that of state-of-the-art SPR sensors.

#### Acknowledgments

This project has been funded in whole or in part with Federal funds from the National Cancer Institute, National Institutes of Health, under award 1 R21 RR021893. One of the authors Yunbo Guo was supported by Riethmiller Fellowship of the University of Michigan.